



Effect of ammonium polyphosphate/cobalt phytate system on flame retardancy and smoke & toxicity suppression of rigid polyurethane foam composites

Bing Zhang¹ · Zhaohe Feng² · Xiangxiang Han¹ · Bibo Wang³ · Sujie Yang¹ · Depeng Chen¹ · Jianwen Peng⁴ · Yadong Yang¹ · Xiuyu Liu^{1,5} · Gang Tang^{1,4}

Received: 6 April 2021 / Accepted: 20 September 2021 / Published online: 6 October 2021
© The Polymer Society, Taipei 2021

Abstract

Rigid polyurethane foam/ammonium polyphosphate/cobalt phytate (RPUF/APP/PA-Co) composites were prepared by one-step water-blown method using ammonium polyphosphate (APP)/cobalt phytate (PA-Co) as a flame retardant system. The char residue of RPUF/APP/PA-Co increased significantly than that of RPUF, indicating that the thermal stability of composites was enhanced. Cone calorimetry and smoke density tests showed that when 40 phr APP and 10 phr PA-Co were added, the total heat release and smoke release of RPUF/APP40/PA-Co10 composite decreased significantly. TG-IR test confirmed that APP/PA-Co could significantly inhibit the release of flammable gases (hydrocarbons, esters) and toxic gases (aromatic compounds, isocyanate, CO, HCN,) of RPUF/APP/PA-Co composites and improve the fire resistance of composites. SEM-EDS, Raman spectra and FTIR were applied to investigate the char residues of composites. The results showed that APP/PA-Co loading was beneficial to the generation of dense char layer with high degree of graphitization and reducing the release of combustible substances and smoke of composites.

Keywords Rigid polyurethane foam · Ammonium polyphosphate · Cobalt phytate · Smoke & toxicity suppression · Fire safety

Introduction

As an important polymer, polyurethane is widely used in building insulation, automobile components and chemical pipelines. Rigid polyurethane foam (RPUF) is usually used

in household appliances and building materials due to its good mechanical properties and thermal insulation properties [1–3]. Nevertheless, RPUF has two fatal disadvantages. First, RPUF is flammable and releases much heat instantly because of its organic skeleton and porous structure. Second, once ignited, RPUF will produce much smoke and toxic gases [4, 5]. The above deficiencies are a major obstacle to the safe use of RPUF. Therefore, it is necessary to modify RPUF.

Reactive type and additive type are the two main flame retardant strategies of RPUF [6]. The reactive flame-retardant method is to prepare intrinsic flame-retardant RPUF with phosphorous-containing polyol as a flame retardant precursor. Due to the stable chemical bonds between flame-retardant elements and polyurethane molecular chains, its flame retardant efficiency is high without migration in the long service of the materials [7]. However, the preparation cost of this method is high, and the shrinkage inevitably occurs in the foaming process, which affect the later use of products [8, 9]. Additive type flame retardant RPUF is often prepared by adding flame retardant particles into RPUF matrix. At present, the additive flame retardant method is still the common strategy for fabricating flame retardant RPUF

✉ Xiuyu Liu
cristalliu@163.com

✉ Gang Tang
tanggang@ahut.edu.cn

¹ School of Architecture and Civil Engineering, Anhui University of Technology, 59 Hudong Road, Ma'anshan, Anhui 243002, China

² Hangzhou Steam Turbine Company Limited, 1188 Dongxin Road, Hangzhou 310022, Zhejiang, China

³ State Key Laboratory of Fire Science, University of Science and Technology of China, 96 Jinzhai Road, Hefei 230026, Anhui, China

⁴ ASAP Technology (JiangXi) Co., Ltd, Ji'an 343000, Jiangxi, China

⁵ Nanjing Gongda Kaiyuan Environmental Protection Technology (Chuzhou) Co., Ltd, Chuzhou 239000, Anhui, China

composites because of its simple preparation process and controllable conditions [10].

Ammonium polyphosphate (APP) has become one of the most popular phosphorus-containing intumescent flame retardant due to its low toxicity, low smoke and high flame retardancy, which is often used in the flame retardancy of various polymer [11, 12]. Barikani et al. [13] studied the effects of APP, melamine cyanurate (MCA), aluminum hydroxide (ATH), borax and expanded graphite (EG) on the compressive strength and fire resistance of RPUF. They found that APP was the most excellent flame retardant. Meng et al. [14] combined APP and EG for preparing flame retardant RPUF composites. When the additive amount was 15 wt% (APP: EG=1:1), the LOI of composites reached 30.5 vol%. Li et al. [15] prepared PMAPP by modifying APP with polymethyl methacrylate (PMMA), which was further introduced to RPUF. When the addition amount of PMAPP was 25 wt%, the LOI of composites enhanced to 25.3 vol%, and the pHRR decreased by 33.7%. Although the loading of APP effectively enhanced the flame retardancy of composites, the compatibility of APP particles with polymer matrix was poor. At the same time, it also increased the smoke and toxic gases generated by the composites, which worsened its mechanical properties and fire safety [16, 17]. Therefore, the best solution is to explore a novel flame retardant system with superior smoke & toxicity suppression and flame retardancy.

Compared with synthesising new flame retardants, the development of a synergistic system was relatively simple and cheap. Phytate metal salts had good smoke suppression and toxicity reduction effect, good compatibility with matrix, and cobalt ion had excellent catalytic oxidation effect [18, 19]. Here, this work introduced cobalt phytate (PA-Co) as a synergist, which was combined with APP to form APP/PA-Co flame retardant system, endowing RPUF composites high flame retardancy with excellent smoke & toxicity suppression. This system provided a novel strategy for fabricating fire retarded RPUF composites with low flame retardant loading and low cost. The effects of APP/PA-Co system on the flame retardancy, combustion performance, thermal stability, smoke & toxicity suppression of RPUF/APP/PA-Co

composites were systematically investigated by a series of test methods. On this basis, the mechanism of RPUF/APP/PA-Co composites was systematically analyzed.

Experimental section

Experimental materials

Polyether polyol (LY-4110) and triethylene diamine (A33, 33%) were purchased by Jiangsu Lvyuan New Material Technology Co., Ltd, China, Polyaryl polymethylene isocyanate (PAPI) was provided by Wanhua Chemical Group Co., Ltd, China, Dibutyltin dilaurate (LC) was purchased from American Air Chemical Co., Ltd., Silicone surfactant (AK-8805) was provided from Jining Hengtai Chemical Co., Ltd, China, Triethanolamine (TEOA) was purchased from China National Pharmaceutical Group Chemical Reagent Co., Ltd., Ammonium polyphosphate (APP), industrial-grade, was purchased from Jinan Fine Chemical Co., Ltd, China, Cobalt phytate (PA-Co) was prepared according to the literature [18]. Distilled water was produced in the laboratory.

Preparation of RPUF composites

As shown in Table 1, LC, LY-4110, AK-8805, A33, TEOA, distilled water, APP and PA-Co were added into a 1000 ml beaker according to the experimental ratio, which was quickly stirred evenly with a blender. Then, the PAPI with the given proportion was quickly poured into the mixture system and continued to stir for about 10 s. When bubbles appeared, poured the mixture into a mold quickly, foamed naturally, and then cured it at 80 °C for 6 h. The samples were cut as required for the experiment.

Measurement and characterization

Oxford Aztec X-Max 80 energy dispersive X-ray spectrometer (EDS) (UK) combining with SU8220 scanning electron

Table 1 The formulae of RPUF composites

Sample	RPUF	RPUF/APP49/ PA-Co1	RPUF/APP47/ PA-Co3	RPUF/APP45/ PA-Co5	RPUF/APP40/ PA-Co10	RPUF/ APP50
LY-4110 (g)	100	100	100	100	100	100
PM-200 (g)	150	150	150	150	150	150
LC (g)	0.5	0.5	0.5	0.5	0.5	0.5
AK-8805 (g)	2	2	2	2	2	2
A33 (g)	1	1	1	1	1	1
TEOA (g)	3	3	3	3	3	3
Water (g)	2	2	2	2	2	2
APP (g)	0	49	47	45	40	50
PA-Co (g)	0	1	3	5	10	0

microscope (SEM) (JEOL Ltd, Japan) was applied to scrutinize the morphology of char residues and the cell structure of RPUF/APP/PA-Co composites. The accelerating voltage was 20 kV. The composites were sprayed with a thin layer of conductivity earlier than observation to enhance the conductivity.

According to GB/T10297-2015, the thermal conductivity of composites with sample size of 50 mm×50 mm×25 mm was tested using the TC3000E thermal conductivity instrument (Xi'an Xiayi Electronic Technology Co., Ltd, China). Each group was tested three times, and the average value was calculated.

According to GB/T6343-2009, the density of composites was calculated according to sample weight/sample volume with sample size of 50 mm×50 mm×50 mm. Each group was tested three times to calculate the average value.

The thermal stability analysis of composites was carried out with Q5000IR (TA, USA) thermal analyzer. Nitrogen conditions, heating rate 20 °C/min, heating from room temperature to 800 °C. The temperature corresponding to a sample weight loss of 5 wt% was taken as the initial degradation temperature ($T_{-5\%}$).

According to ASTM-D2863 standard, JF-3 oxygen index instrument (Jiangning Analytical Instrument Co., Ltd, China) was used to test the limiting oxygen index (LOI) of RPUF/APP/PA-Co composites. The size of samples was 127 mm×10 mm×10 mm.

According to GB/T2408 standard, CZF-3 (Jiangning Analytical Instrument Co., Ltd, China) horizontal and vertical combustion tester were used to test the vertical combustion grade of composites. The sample size was 125 mm×13 mm×10 mm.

Cone calorimeter 6180 (Siemens analyzer) was used to test the combustion properties of composites according to ISO5660-1 standard. The radiation flux was 35 kW/m² and the sample size was 100 mm×100 mm×25 mm.

According to GB/T8627-2007 standard, the smoke density of composites was tested by JCY-2 smoke density tester. The sample size was 25.5 mm × 25.5 mm × 6.2 mm. Each sample was subjected to three parallel experiments and their mean values were calculated.

Thermogravimetric analysis-Fourier Transform Infrared spectrometer (TG-FTIR) was applied to analyze pyrolysis gas products of the composites by 209F3 thermogravimetric analyzers (Netzsch, Germany) connecting to TENSOR infrared analyzer (Bruck, Germany). 5-10 mg samples were put into an alumina crucible, heated from 40 °C to 800 °C in nitrogen atmosphere at a heating rate of 20 °C/min.

Raman spectra of char residues were collected by LABRAM-HR Confocal Raman spectrometer (HORIBA Jobin Yvon).

Results and discussion

Cell structure

As can be seen from Fig. 1a, RPUF cells were relatively uniform. When 50 phr APP was added, as shown in Fig. 1f, the cells were damaged, with reduced uniformity and particles precipitation. This may be due to the limited compatibility between RPUF matrix and APP. High flame retardant loading increased local viscosity of the composites in the foaming process, which promoted the agglomerate of APP particles in the matrix. Meanwhile, APP particles penetrated the cell wall and destroyed cell structure. When 1 phr PA-Co and 49 phr APP were added, the fracture surface of the RPUF/APP49/PA-Co1 composite became smooth, and the degree of cell damage was reduced. With the addition of PA-Co, the uniformity of cells was improved. When 5 phr PA-Co was added, the uniformity and pore size of cells were almost similar to RPUF, which may be because PA-Co was a bio-based flame retardant, which enhanced the compatibility between APP/PA-Co flame retardant system and matrix. It could be seen from Fig. 1e that there was inconspicuous APP precipitation on the surface of the RPUF/APP40/PA-Co10 composite with the thinner cell wall, which may be because P-OH in PA-Co reacted with isocyanate, which released a large amount of CO₂ gas at the initial stage of foaming.

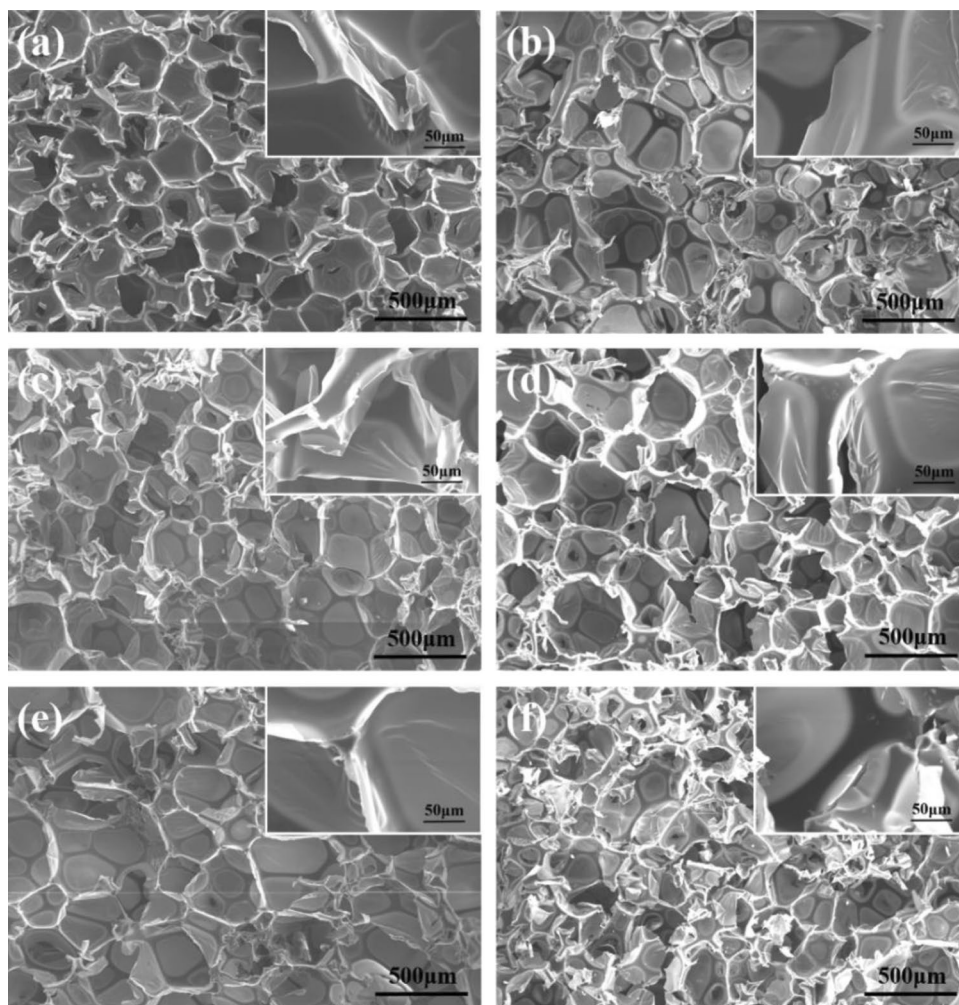
Physical properties

As shown in Table 2, the thermal conductivity of RPUF was 0.0390 W/m·K and the density of RPUF was 54.9 kg/m³. When 50 phr APP was loaded, the density of RPUF/APP50 reached 56.7 kg/m³, and the thermal conductivity was 0.0404 W/m·K. It was mainly because of higher thermal conductivity and density of APP than RPUF matrix. At the same time, the compatibility between matrix and APP was poor, and some cell structures were destroyed, which further increased the density and thermal conductivity. With the increase of PA-Co addition, the density of composites decreased gradually. However, the thermal conductivity of composites decreased first and then increased. It may be because that the increase of PA-Co content increased CO₂ production and promoted foaming, resulting in thinner cell walls even open cell structure and thus increasing the thermal conductivity. On the whole, the thermal conductivity of RPUF/APP/PA-Co composites was relatively low.

Thermal stability

Figure 2 showed the thermogravimetric analysis of RPUF and RPUF/APP/PA-Co composites in nitrogen atmosphere. Table 3 showed the data results. The degradation of

Fig. 1 SEM images of fracture surface of RPUF composites: (a) RPUF; (b) RPUF/APP49/PA-Co1; (c) RPUF/APP47/PA-Co3; (d) RPUF/APP45/PA-Co5; (e) RPUF/APP40/PA-Co10; (f) RPUF/APP50



the composites was divided into two stages. The first stage was the degradation of the hard segment of polyurethane molecular chain, and the second stage corresponded to the degradation of its soft segment [20, 21]. For RPUF, the first degradation stage was 200–415 °C, and the second degradation stage was 415–600 °C. When APP/PA-Co was added, the range of the first degradation stage of RPUF/APP/PA-Co composites was reduced to 200–390 °C, while the range of the second degradation stage of composites was increased to

390–600 °C. The $T_{-5\%}$ of RPUF/APP50 decreased to 251 °C compared with RPUF. The temperature (T_{\max} : the maximum degradation rate of the first stage) decreased to 308 °C, which was mainly due to acidic substances (such as polyphosphoric acid) produced by APP decomposition promoted the degradation of polyurethane molecular chains [22]. With the increase of PA-Co loading, the $T_{-5\%}$ of composites showed a further downward trend, which indicated that APP/PA-Co system promoted the degradation of the composites at the initial stage. However, the $T_{-50\%}$ of RPUF/APP50 and RPUF/APP40/PA-Co10 were 347 °C and 363 °C, respectively, which were significantly enhanced than that of RPUF, indicating that RPUF/APP/PA-Co composites had higher thermal stability. At 700 °C, the char residue of RPUF/APP50 was 31.6wt%, which was significantly increased compared with 12.3wt% of RPUF. With PA-Co addition, the char residues of RPUF/APP40/PA-Co10 was up to 35.2wt%. The above results confirm synergistically effect in APP/PA-Co system improves the thermal stability of RPUF composites at high temperature.

Table 2 Typical physical performance parameters of RPUF/APP/PA-Co composites

Sample	ρ /(kg/m ³)	λ /(W/m·K)
RPUF	54.9±3.1	0.0390±0.0004
RPUF/APP49/PA-Co1	55.8±2.3	0.0434±0.0006
RPUF/APP47/PA-Co3	53.5±5.0	0.0424±0.0003
RPUF/APP45/PA-Co5	52.8±3.1	0.0403±0.0003
RPUF/APP40/PA-Co10	51.5±2.1	0.0444±0.0007
RPUF/APP50	56.7±1.2	0.0404±0.0004

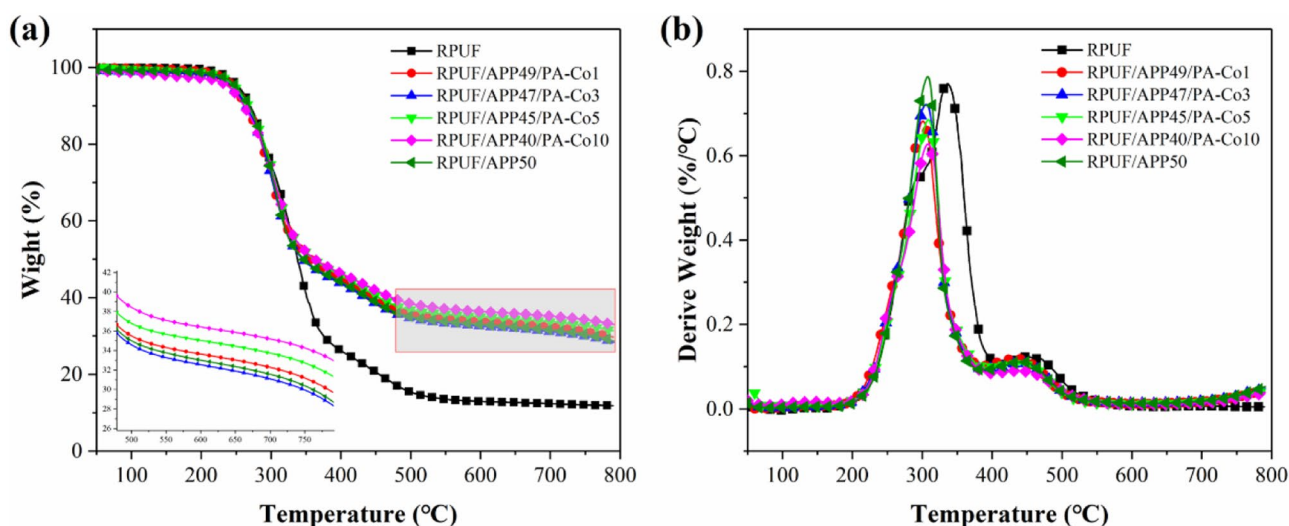


Fig. 2 TG (a) and DTG (b) curves of RPUF composites

Flame retardancy

Limiting oxygen index (LOI) and vertical combustion test were applied to investigate flame retardancy of the composites. In Fig. 3, the LOI of RPUF was 18.8 vol% and there was no rating in UL-94 test. When 50 phr APP was loaded, the LOI of RPUF/APP50 was increased to 23.7 vol% with V0 level in UL-94 test, indicating that the addition of APP significantly enhanced the flame retardancy of the composite. This is because polyphosphoric acid produced by APP degradation can catalyze the polymer chain to form char, and inhibit the further combustion of composites. However, the LOI of composites did not change much with the addition of PA-Co, and UL-94 V0 level was still reached.

Combustion properties

Cone calorimetry is a common way to characterize the combustion behavior of polymer [23–25]. As shown in Fig. 4, the combustion performance of RPUF, RPUF/APP50 as well as RPUF/APP40/PA-Co10 composites were tested by cone calorimetry. Corresponding data were shown in Table 4. Due to the premature degradation

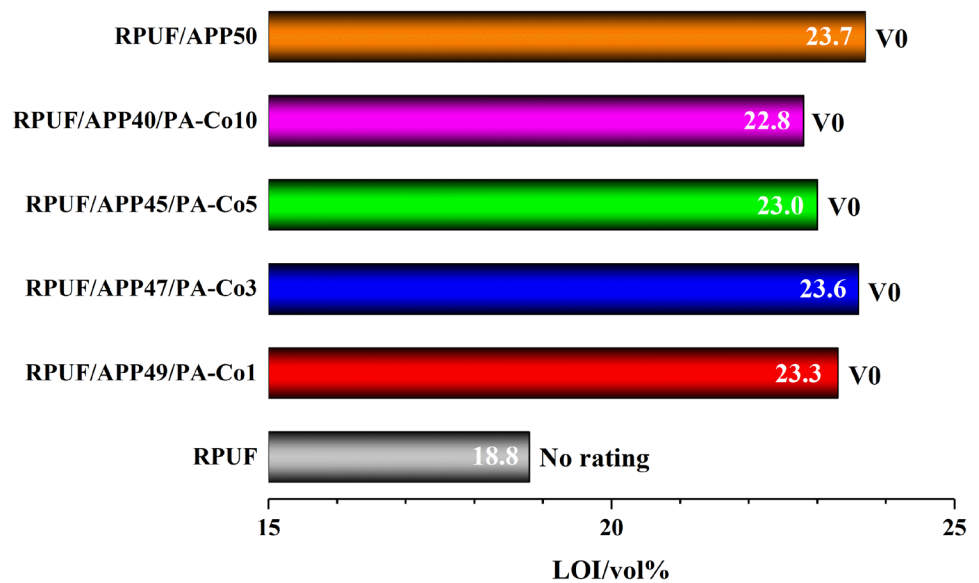
of the unstable carbamate structure in the polyurethane molecular chain, the composites were quickly ignited in a short time. It could be found that RPUF had only one heat release peak in the whole combustion process, showing typical combustion characteristics of organic materials without flame retardancy. RPUF/APP50 and RPUF/APP40/PA-Co10 exhibited multiple low-intensity heat release processes, which may be due to the further degradation of unstable char layer formed by catalyzing carbonization effect of APP and APP/PA-Co system. In Fig. 4a, the peak heat release rate (pHRR) of RPUF was 260.7 kW/m². When 50 phr APP was added, the pHRR of RPUF/APP50 decreased to 181.2 kW/m². When 10 phr PA-Co was used to replace APP, the pHRR of RPUF/APP40/PA-Co10 further decreased to 148.2 kW/m². The results showed that APP and PA-Co flame retardant system could effectively reduce the HRR and thus improved the fire safety of composites. The extension of combustion time (T_d) also supported this conclusion.

In Fig. 4b, the total heat release (THR) of RPUF was 23.0 MJ/m², and the THR of RPUF/APP50 and RPUF/APP40/PA-Co10 were 19.3 MJ/m² and 17.4 MJ/m², which were 16.1% and 24.3% lower than that of RPUF, respectively.

Table 3 TGA data of RPUF composites

Sample	$T_{5\%}$ (°C)	$T_{50\%}$ (°C)	T_{max} (°C)		Char residue at 700 °C(wt%)
			Step1	Step2	
RPUF	254	338	336	449	12.3
RPUF/APP49/PA-Co1	246	356	301	433	32.3
RPUF/APP47/PA-Co3	245	346	306	445	31.1
RPUF/APP45/PA-Co5	248	361	309	440	33.7
RPUF/APP40/PA-Co10	239	363	308	437	35.2
RPUF/APP50	251	347	308	443	31.6

Fig. 3 LOI and UL-94 test results of RPUF composites



This may be because PA molecules could produce active free radicals capturing $\cdot\text{OH}$ and $\text{H}\cdot$ free radicals, and the NH_3 and water vapor generated by APP decomposition could dilute combustible gases and inhibit the combustion reaction [26–28].

The Av-EHC (average effective heat of combustion) revealed the degree of combustion of vapor-phase volatiles [29]. The Av-EHC of RPUF/APP50 was 12.2 MJ/kg, which decreased by 18.7% than that of RPUF, suggesting that APP had a quenching effect in the gas phase. For RPUF/APP40/PA-Co10, its Av-EHC was 7.8 MJ/kg, which was 36.1% lower than that of RPUF/APP50, indicating an excellent quenching effect of APP/PA-Co system.

Smoke was the main factor causing casualties in fire accidents [30]. As shown in Fig. 5a, RPUF/APP40/

PA-Co10 showed the lowest smoke generation rate (SPR) in an early stage of combustion. The SPR of RPUF/APP50 and RPUF/APP40/PA-Co10 was higher than that of RPUF in the later combustion stage, which may be because of further solidification of unstable char layer formed in the early stage. From Fig. 5b–d, it could be seen that simply adding APP could not effectively reduce TSP (total smoke production) and TSR (total smoke release) of RPUF/APP50 but reduced the smoke factor (SF: the product of pHRR and TSR) and smoke parameters (SP: the product of pHRR and SEA) of composites, indicating that the smoke suppression effect of APP was limited. When 10 phr PA-Co and 40 phr APP were added, the TSP and TSR of RPUF/APP40/PA-Co10 decreased significantly. And the TSR of RPUF/APP40/PA-Co10 was decreased by 41.2%

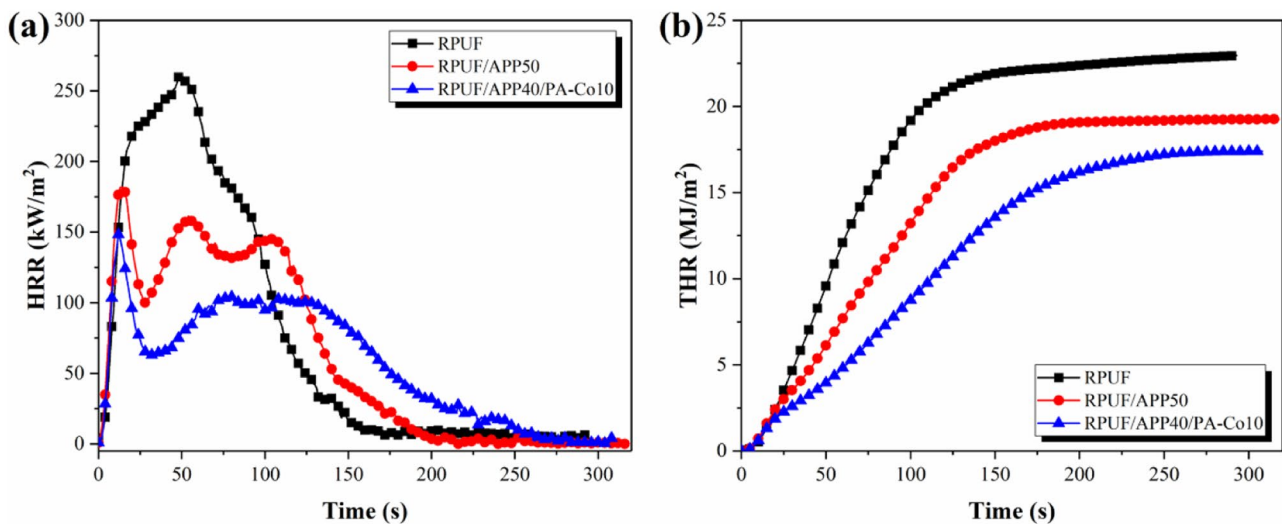


Fig. 4 HRR and THR curves of RPUF composites: (a) HRR; (b) THR

Table 4 Cone calorimetry data of RPUF composites

Sample	RPUF	RPUF/APP50	RPUF/ APP40/ PA-Co10
TTI (s)	2	2	2
T _p (s)	49	13	11
T _d (s)	154	201	250
pHRR (kW/m ²)	260.7	181.7	148.2
THR (MJ/m ²)	23.0	19.3	17.4
TSP (m ²)	3.8	3.6	2.2
TSR (m ² /m ²)	422.63	403.69	248.38
Av-EHC (MJ/kg)	15.0	12.2	7.8
Av-SEA(m ² /kg)	178.3	116.0	44.3
MLR (g/s·m ²)	9.6	7.1	4.6
CY (wt%)	23.2	31.6	40.4
FPI (m ² ·s/kW)	0.0077	0.0110	0.0135
SF (MW/m ²)	110.2	73.3	36.8
SP (MW/kg)	46.5	21.1	6.6

compared with RPUF, indicating that APP/PA-Co system endowed the composite with excellent smoke suppression property. This may result from the gas products generated by the pyrolysis of APP/PA-Co promoted polyurethane chain to form dense carbon structure, inhibiting the escape of smoke particles [31].

The fire performance index (FPI) could emerge fire safety performance of polymer composites [32]. The FPI of RPUF/APP50 and RPUF/APP40/PA-Co10 were 0.0110 m²·s/kW and 0.0135 m²·s/kW, respectively, which were greatly improved compared with RPUF, suggesting less fire hazard of the composites.

CO is an important deadly toxic gas in fires [33, 34]. Figure 5e showed the CO yield curve of composites. The addition of APP increased CO production of RPUF/APP50 in the initial stage. However, RPUF/APP40/PA-Co10 maintained a low CO yield during the entire combustion process. The main reason was that APP/PA-Co system reduced the degree of combustion of RPUF/APP40/PA-Co10. Furthermore, Co ions could adsorb CO and convert it into CO₂ through catalytic oxidation, thus reducing CO [35].

Figure 5 (f) showed the mass versus time curves of composites during the test. The results showed that the mass of RPUF decreased rapidly after ignition, and final char residues was 23.2wt %, and the mass-loss rate (MLR) in the whole process was 9.6 g/s·m². The mass curves of RPUF/APP50 and RPUF/APP40/PA-Co10 were above RPUF, showing a low degradation rate. Among them, RPUF/APP40/PA-Co10 possessed the lowest degradation rate with MLR of 4.6 g/s·m² and the highest char residues of 40.4 wt%, which was mainly due to that the Co ions could effectively retain gaseous products into condensed phase.

The photos of char residues after cone calorimetry test were shown in Fig. 6. The char layer of RPUF had many cracks on the surface with relatively loose char residue. This structure could not effectively restrain the heat and mass transfer during combustion, so RPUF had higher THR and TSR. The char layer of RPUF/APP50 composite was relatively thick and dense with no cracks appearing on the surface, but there were still some holes. When 10 phr PA-Co and 40 phr APP were added, the holes disappeared, and the char layer became thicker and denser. Such structure effectively inhibited the release of volatile products, thus endowed with enhanced fire performance of RPUF/APP40/PA-Co10 composite.

Smoke density

Figure 7 showed the smoke density test of composites. The data were shown in Table 5. Compared with RPUF, the maximum smoke density (MSD) and smoke density grade (SDR) of RPUF/APP50 were decreased from 68.94% and 40.06 to 58.09% and 39.74, respectively. The inconspicuous decrease of MSD for RPUF/APP50 indicated limited smoke suppression performance of APP to the composites. SDR and MSD and of RPUF/APP40/PA-Co10 were reduced to 50.56% and 33.77 compared with RPUF, which were reduced by 26.7% and 15.7%, respectively, suggesting excellent smoke suppression effect was observed in RPUF/APP40/PA-Co10. The above results indicated that APP/PA-Co system had excellent smoke suppression effect in RPUF composite.

Analysis of gas-phase products

In an anaerobic environment, the polymer matrix continuously released gas products in the process of thermal degradation, so the release of gas products during polymer degradation was detected by TG-FTIR. [36]. Figure 8 showed the 3D spectra of the release of gas-phase products of the composites. The gas-phase products were mainly distributed in the range of 3700-3800 cm⁻¹, 3300-3400 cm⁻¹, 2800-3050 cm⁻¹, 2500-2400 cm⁻¹, 1500-1800 cm⁻¹, 1100-1300 cm⁻¹ and 650-750 cm⁻¹. Meanwhile, the new band appeared within 900 cm⁻¹-1000 cm⁻¹. Figure 9 was the infrared spectra of the gas-phase product of the composites at the maximum thermogravimetric rate, in which the absorption peak of RPUF/APP50 and RPUF/APP40/PA-Co10 at 966 cm⁻¹ corresponded to NH₃ generated by the degradation of APP [37].

The Gram-Schmidt curve and typical pyrolysis gas intensity curves of the composites were shown in Fig. 10. It could be seen from the G-S curves that the pyrolysis of the composites was divided into two stages. In the whole pyrolysis process, the G-S curves of RPUF/APP50 and RPUF/APP40/PA-Co10 were lower than that of RPUF, and the overall G-S strength intensity of RPUF/APP40/PA-Co10 was the

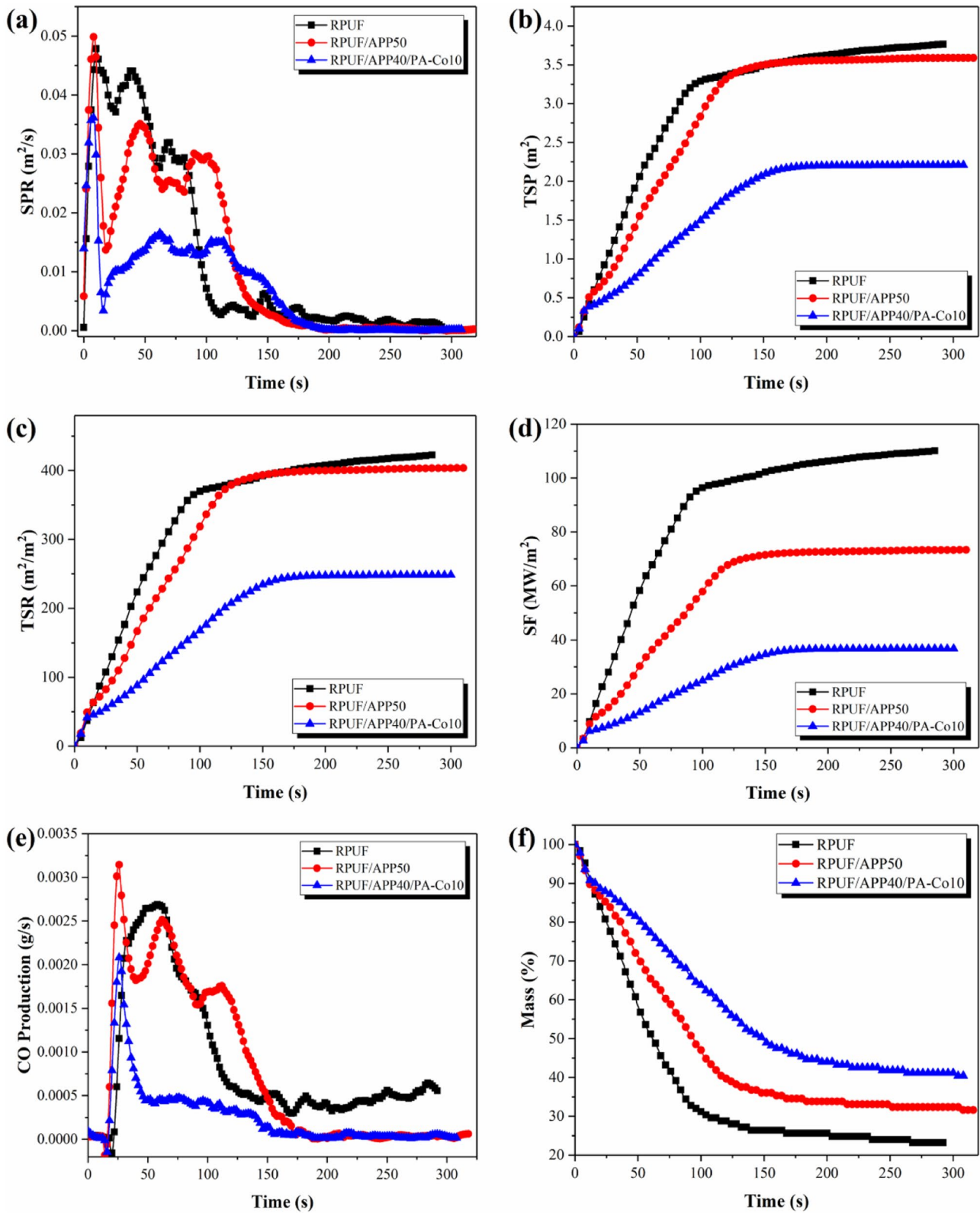
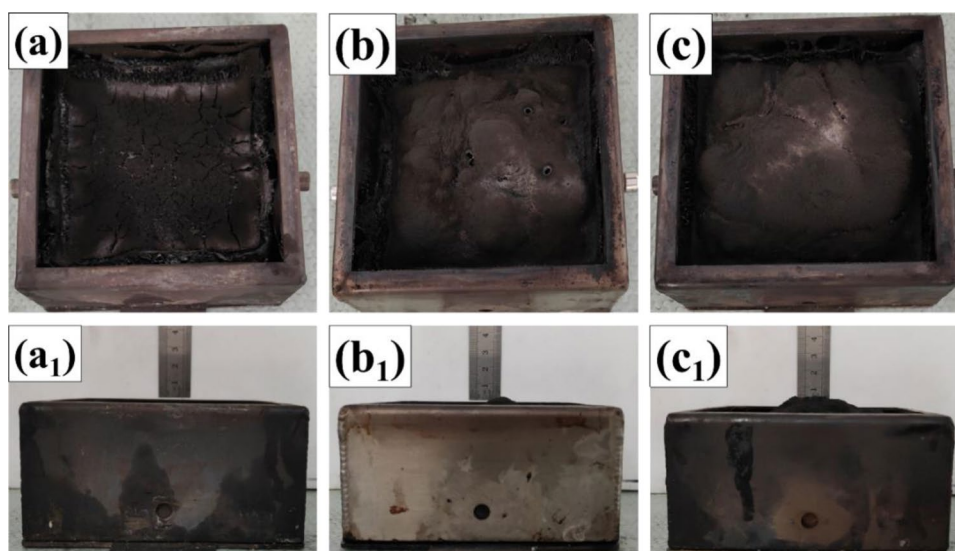


Fig. 5 SPR, TSP, TSR, SF, COP and Mass curves of RPUF composites: (a) SPR; (b) TSP; (c) TSR; (d) SF; (e) COP; (f) Mass

Fig. 6 Photos of char residues of RPUF (**a, a1**), RPUF/APP50 (**b, b1**) and RPUF/APP40/PA-Co10 (**c, c1**) composites after cone calorimetry



lowest. Compared with RPUF, RPUF/APP50 showed a significant decrease in toxic gases (isocyanates and aromatic compounds) and flammable gases (hydrocarbons and esters), which indicated that APP could inhibit gases released during combustion. The gas products release intensity of RPUF/APP40/PA-Co10 was further reduced and the peak of gas products were delayed, indicating synergistic effect between APP and PA-Co, which significantly inhibited the release of gas products for the RPUF composites. CO and HCN were important factors causing death in polyurethane fires. Even a small amount of CO intake would cause poisoning, and the toxicity of HCN was about 20 times that of CO, which could inhibit the action of human cells on oxygen [36]. The above results showed that APP combined with

PA-Co could significantly reduce the release of HCN and CO, thus improving the fire resistance of the composites.

Char residues analysis

The char residues of the composites were further investigated by SEM, while the influence of APP/PA-Co on the fire prevention, smoke and toxicity suppression of composites was clarified. In Fig. 11, the char layer of RPUF was loose with many cracks. When 50 phr APP was added, the char layer became smooth and compact, but there were still a few pores. According to Fig. 11b–d, it could be observed that there was a thick and expansive char layer with some pore structure. In Fig. 11e, the compactness of the char layer for RPUF/APP40/PA-Co10 was significantly improved, without any holes and cracks. Fig. 11a1 revealed that large pore structure and char residue fragments were on the inner surface of RPUF char layer. Moreover, the inner char residue of RPUF/APP/PA-Co presented a typical honeycomb structure due to the influence of volatiles generated during combustion [38, 39]. The honeycomb char layers of RPUF/APP50 was the most obvious, which may be due to the release of a large amount of non-combustible NH_3 during APP pyrolysis, diluting combustible gas and removing part of heat. This explained why RPUF/APP50 possessed the highest LOI, but it also damaged the compact char layer to some extent.

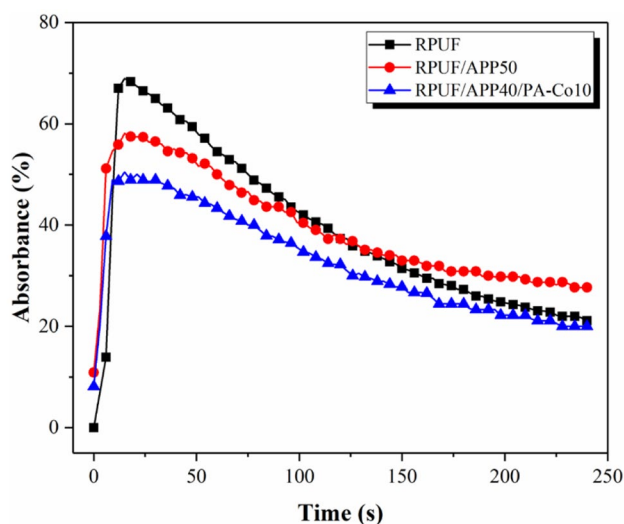


Fig. 7 Absorption rate-time curve of RPUF composites

Table 5 MSD and SDR of RPUF composites

Sample	MSD (%)	SDR
RPUF	68.94	40.06
RPUF/APP50	58.90	39.74
RPUF/APP40/PA-Co10	50.56	33.77

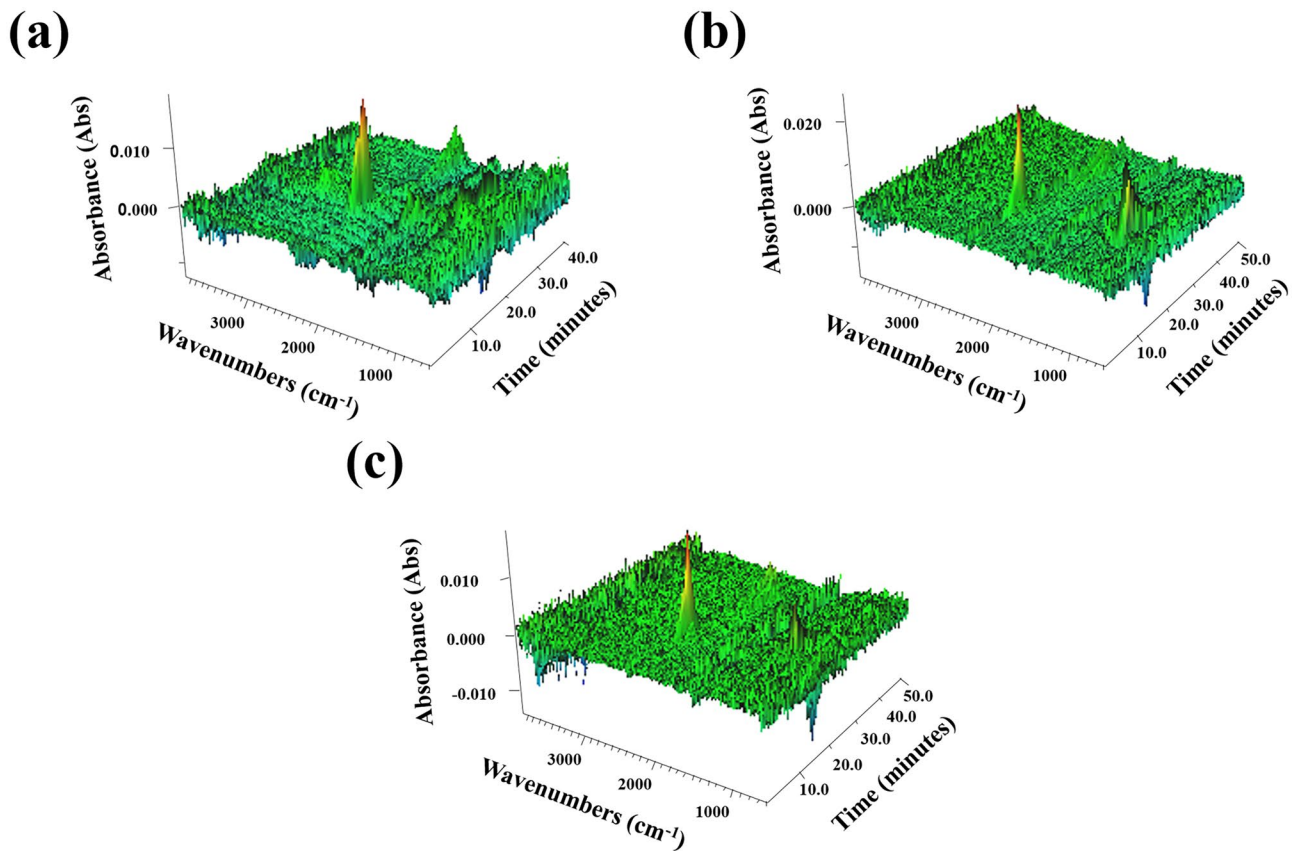


Fig. 8 3D spectra of RPUF composites: (a) RPUF; (b) RPUF/APP50; (c) RPUF/APP40/PA-Co10

The inner and outer char layers of RPUF/APP50 and RPUF/APP40/PA-Co10 were further characterized by EDS. It could be seen from Fig. 12a, b that RPUF/APP40/

PA-Co10 exhibited higher C content and C/O ratio than those of RPUF/APP50, indicating that RPUF/APP40/PA-Co10 had higher oxidation resistance [40]. The difference in C/O ratio on the inner surface of composites was not significant, indicating that PA-Co mainly acted on the char layer outer surface. Meanwhile, the uniform distribution of P and Co elements in the char layers inner and outer surfaces indicated that APP and PA-Co could degrade to form P-Co-C complex in condensed phase and played a flame-retardant role [38].

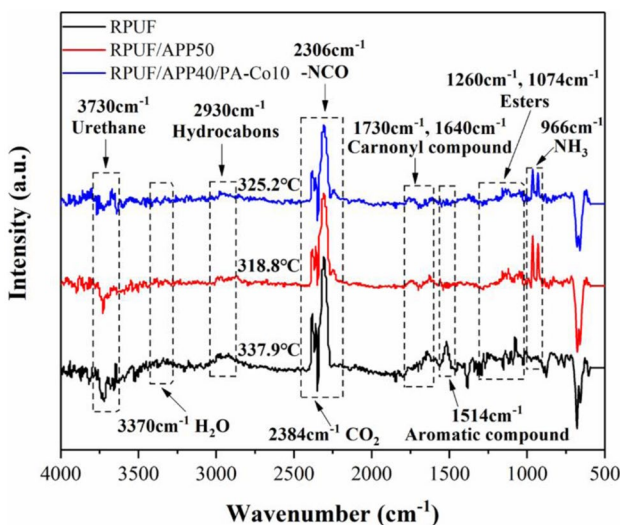
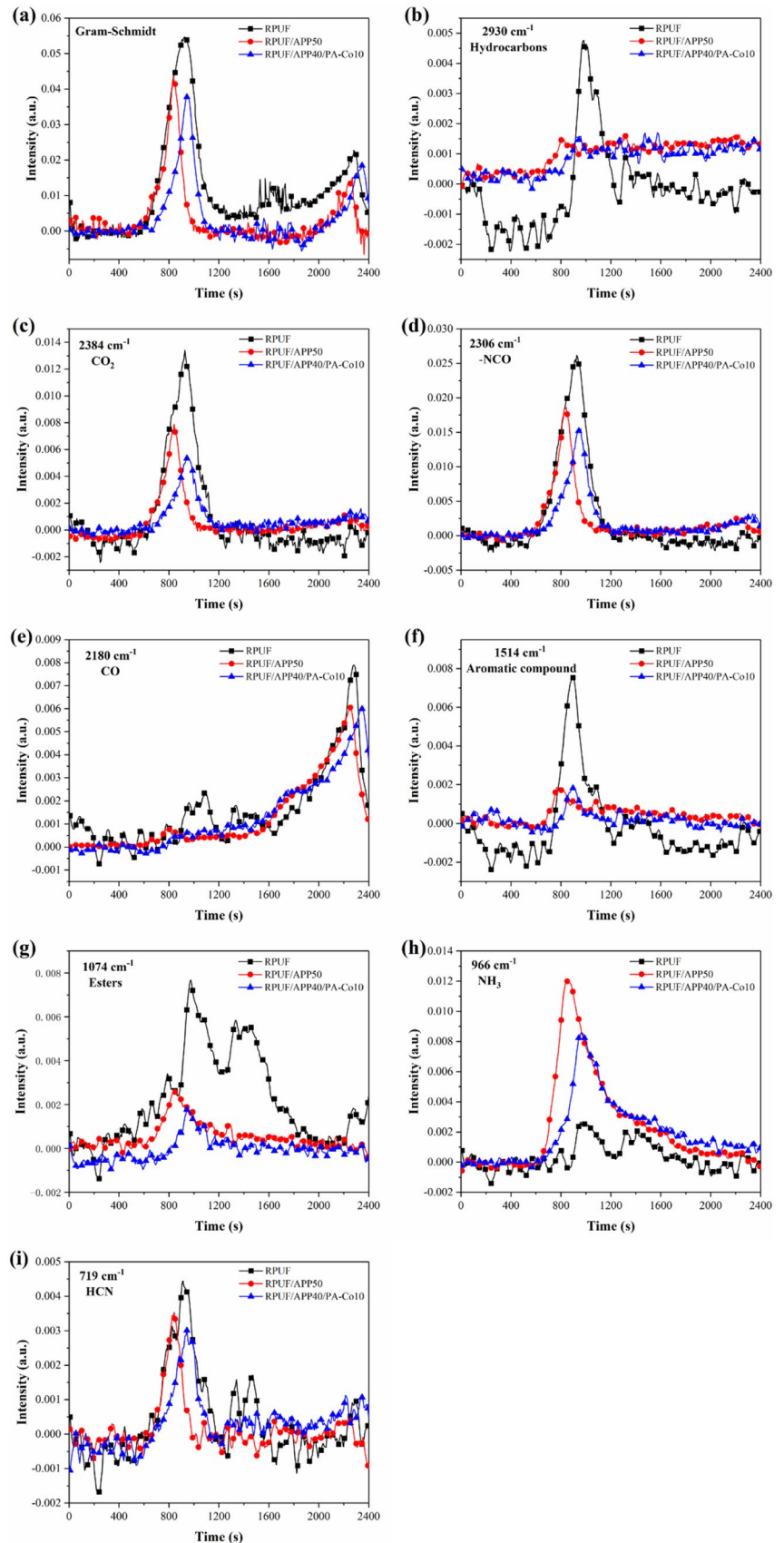


Fig. 9 Infrared spectra of gas-phase products at maximum thermogravimetric rate of RPUF composites

Raman spectroscopy was a commonly used method to characterize carbonaceous materials. The graphitization degree of char residues could be measured by the area ratio of D band to G band (I_D/I_G). The higher the ratio, the lower the graphitization degree, indicating that the materials had worse heat and corrosion resistance [41–43]. In Fig. 13, the I_D/I_G value for RPUF was 2.60, while that of RPUF/APP50 was 2.52. And the I_D/I_G value of RPUF/APP/PA-Co composites further decreased with the increase of PA-Co addition, indicating that APP and PA-Co were helpful to the formation of graphite carbon, thus enhancing the compactness and heat resistance of char residues.

Fig. 10 RPUF composites pyrolysis gas products intensity curves over time: **(a)** GS; **(b)** Hydrocarbons; **(c)** CO_2 ; **(d)** Iso-cyanate compound; **(e)** CO; **(f)** Aromatic compound; **(g)** Esters; **(h)** NH_3 ; **(i)** HCN



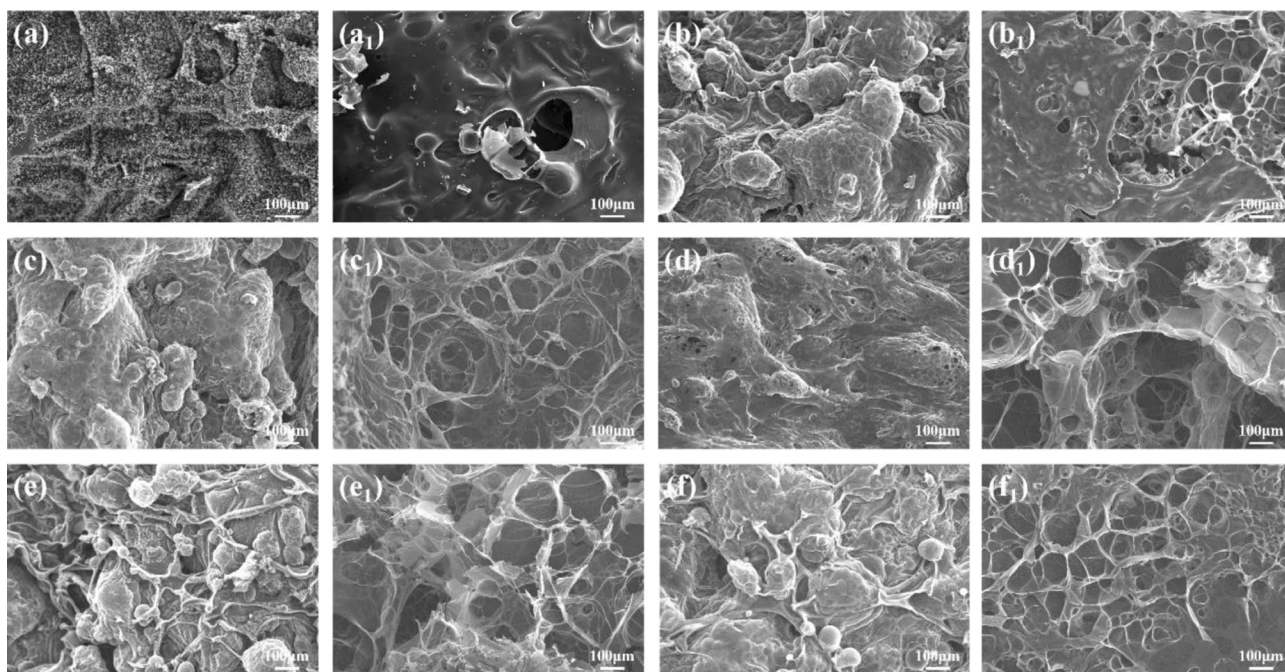


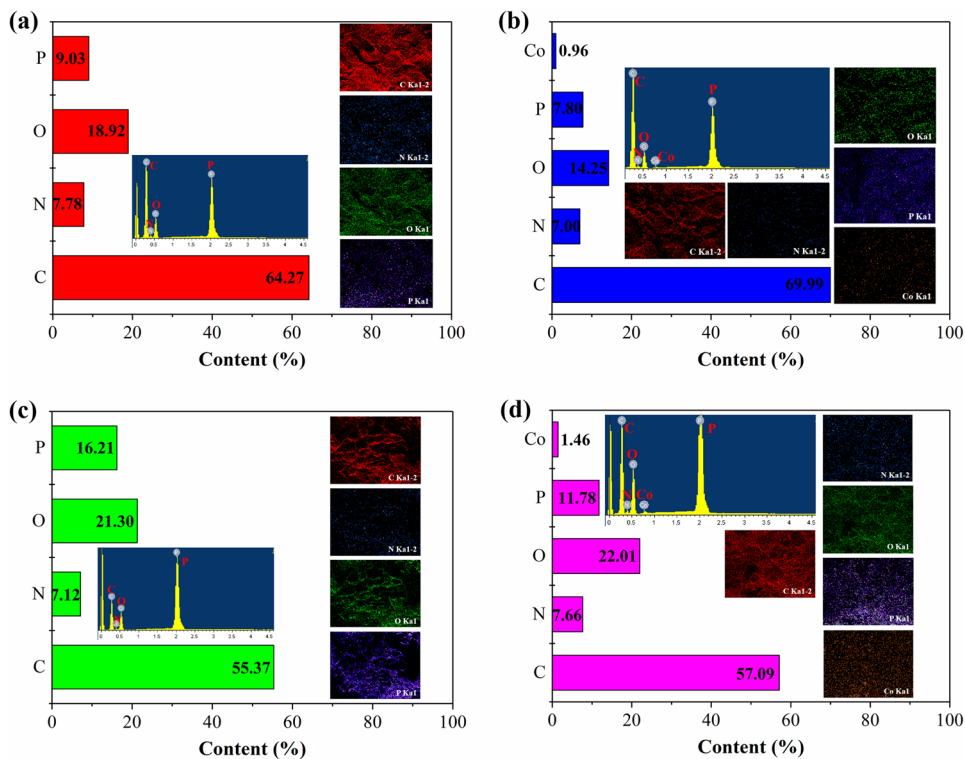
Fig. 11 SEM photographs of char residues inner and outer surface for RPUF composites: (a, a1) RPUF; (b, b1) RPUF/APP49/PA-Co1; (c, c1) RPUF/APP47 /PA-Co3; (d, d1) RPUF/APP45/PA-Co5; (e, e1) RPUF/APP40/PA-Co10; (f, f1) RPUF/APP50

Mechanism description

The action mechanism of RPUF/APP/PA-Co composites was described in detail through the above analysis. As shown

in Fig. 14, in the condensed phase, the polyphosphoric acid generated during APP decomposition promoted the degradation of polyurethane molecular chains to form dense char layers. At high temperatures, polyphosphoric acid reacted

Fig. 12 EDS mapping images of char layers inner (c, d) and outer (a, b) surface of RPUF/APP50 (a, c) and RPUF/APP40/PPA-Co10 (b, d)



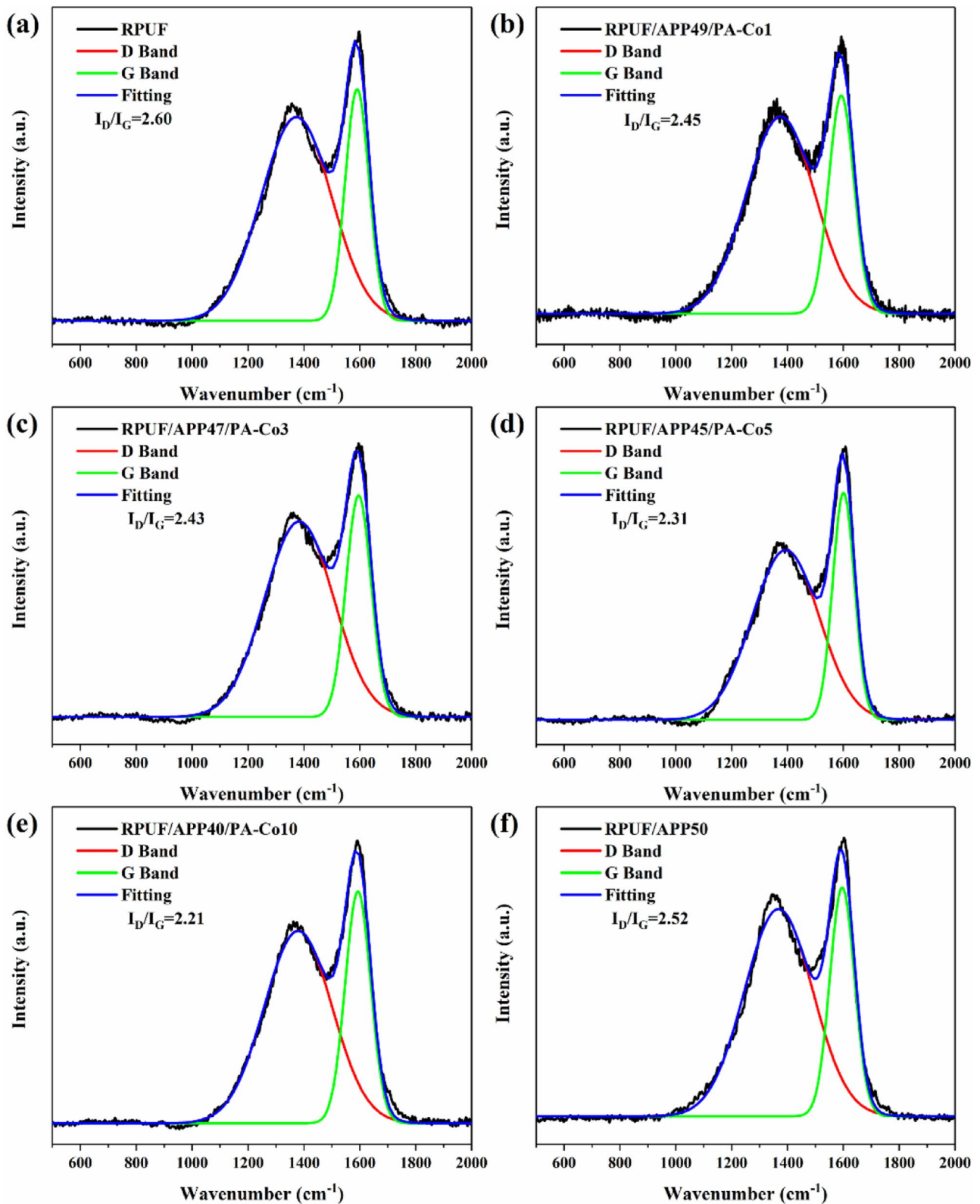
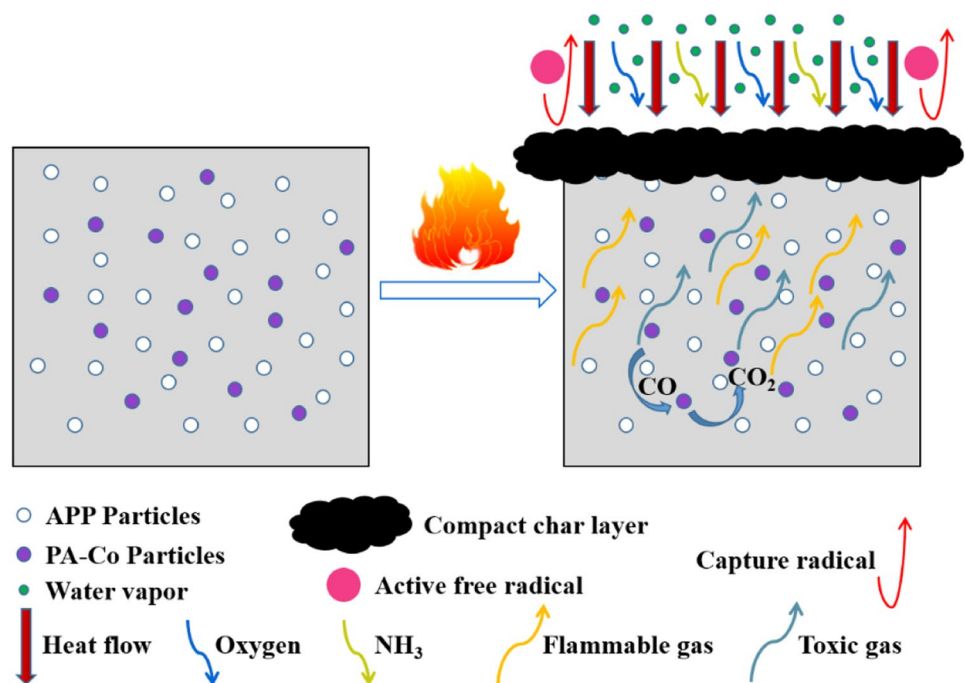


Fig. 13 Raman spectra of RPUF composites: (a) RPUF; (b) RPUF/APP49/PA-Co1; (c) RPUF/APP47/PA-Co3; (d) RPUF/APP45/PA-Co5; (e) RPUF/APP40/PA-Co10; (f) RPUF/APP50

Fig. 14 Schematic diagram for the flame-retardant mechanism of RPUF/APP/PA-Co composites



with isocyanate to form P-O-C compounds. At the same time, pyrophosphate and polyphosphate produced by PA-Co decomposition could catalyze the pyrolysis products of composites into the condensed phase to form carbon, so as to reduce the release of combustibles and flue gases. In the gas phase, PA molecules could produce active free radicals capturing $\cdot\text{OH}$ and $\text{H}\cdot$ active radicals, thus blocking the combustion reaction. Cobalt ion could catalyze the oxidation of CO into CO_2 . At the same time, the decomposition of NH_3 and water vapor produced by APP could dilute combustible gases and remove some heat. In the combustion process, NH_3 could be used as a gas source to promote the expansion of the char layer and inhibit heat and mass transfer. Therefore, the co-effect of the gas-condensed flame retardant mechanism significantly improved the fire resistance of RPUF/APP/PA-Co composites.

Conclusions

RPUF/APP/PA-Co composites were prepared with APP/PA-Co as the flame retardant system. TG test showed that char residue of RPUF/APP40/PA-Co10 was 35.2wt% at 700 °C, which was significantly higher than 12.3wt% of RPUF, confirming that the high temperature thermal stability of RPUF/APP/PA-Co composites was enhanced by the addition of APP/PA-Co. Smoke density tests and Cone calorimetry tests confirmed that APP had limited smoke suppression performance. At the same time, the combined use of APP and PA-Co could effectively weaken the release of smoke, heat, and CO in the combustion of RPUF/APP/PA-Co composites.

TG-FTIR test revealed that APP/PA-Co effectively inhibited the release of flammable gases (hydrocarbons, esters) and toxic gases (isocyanate, CO, aromatic compounds, HCN) during the combustion of composites. SEM, Raman as well as FTIR analysis proved dense char layers with more graphitized carbon structure were formed in the burning of RPUF/APP/PA-Co, which inhibited the transfer of mass and heat. The above results suggested that APP/PA-Co flame retardant system was an excellent choice for modified RPUF composites.

Acknowledgments This work was supported by National Natural Science Fund of China (No. U1833113, 51403004, 51978002), Post-doctoral Science Foundation of China (2017M610399) and Student Research Training Program (SA2000000357).

References

1. Akdogan E, Erdem M, Ureyen ME, Kaky M (2021) Synergistic effects of expandable graphite and ammonium pentaborate octahydrate on the flame-retardant, thermal insulation, and mechanical properties of rigid polyurethane foam. *Polym Compos* 41(5):1749–1762
2. Yang R, Hu WT, Xu L, Song Y, Li JC (2015) Synthesis, mechanical properties and fire behaviors of rigid polyurethane foam with a reactive flame retardant containing phosphazene and phosphate. *Polym Degrad Stabil* 122:102–109
3. Cheng JJ, Ma D, Li SX, Qu WJ, Dong W (2020) Preparation of zeolitic imidazolate frameworks and their application as flame retardant and smoke suppression agent for rigid polyurethane foams. *Polymers* 12(2):347
4. Xu WZ, Wang GS, Xu JY, Liu YC, Chen R, Yan HY (2019) Modification of diatomite with melamine coated zeolitic imidazolate

- framework-8 as an effective flame retardant to enhance flame retardancy and smoke suppression of rigid polyurethane foam. *J Hazard Mater* 379:120819
5. Li A, Yang DD, Li HN, Jiang CL, Liang JZ (2018) Flame-retardant and mechanical properties of rigid polyurethane foam/MRP/mg(OH)₂/GF/HGB composites. *J Appl Polym Sci* 135(31):46551
 6. Han SH, Zhu XD, Chen F, Chen SH, Liu H (2020) Flame-retardant system for rigid polyurethane foams based on diethyl bis(2-hydroxyethyl) aminomethylphosphonate and in-situ exfoliated clay. *Polym Degrad Stabil* 177:109178
 7. Chen L, Chao R, Yang R, Wang YZ (2014) Phosphorus-containing thermotropic liquid crystalline polymers: a class of efficient polymeric flame retardants. *Polym Chem* 5(12):3737–3749
 8. Wang JQ, Chow WK (2005) A brief review on fire retardants for polymeric foams. *J Appl Polym Sci* 97(1):366–376
 9. Yuan Y, Yang HY, Yu B, Shi YQ, Wang W, Song L, Hu Y, Zhang YM (2016) Phosphorus and Nitrogen-Containing Polymers: Synergistic effect on the thermal property and flame retardancy of rigid polyurethane foam composites. *Ind Eng Chem Res* 55(41):10813–10822
 10. Shi XX, Jiang SH, Zhu JY, Li GH, Peng XF (2018) Establishment of a highly efficient flame-retardant system for rigid polyurethane foams based on bi-phase flame-retardant actions. *RSC Adv* 8(18):9985–9995
 11. Gao WY, Wang SJ, Meng FB, Wang YH, Ma HQ (2016) Microencapsulated ammonium polyphosphate with boron-modified phenolic resin. *J Appl Polym Sci* 133(30):43720
 12. Cheng KC, Kuo TH (2020) Flame retardant and mechanical properties of epoxy composites with ammonium polyphosphate and hyperbranched silicon-containing polymers. *J Appl Polym Sci* 137(28):48857
 13. Barikani M, Askari F, Barmar M (2010) A comparison of the effect of different flame retardants on the compressive strength and fire behaviour of rigid polyurethane foams. *Cell Polym* 29(6):343–358
 14. Meng XY, Ling Y, Zhang XG, Tang PM, Tang JH, Ji X, Li ZM (2019) Effects of expandable graphite and ammonium polyphosphate on the flame-retardant and mechanical properties of rigid polyurethane foams. *J Appl Polym Sci* 114(2):853–863
 15. Li SX, Zhou Y, Cheng JJ, Ma QY, Zhang F, Wang Y, Liu M, Wang D, Qu WJ (2020) Mechanical property improvement and fire hazard reduction of ammonium polyphosphate microencapsulated in rigid polyurethane foam. *J Appl Polym Sci* 137(4):48307
 16. Wang SW, Shi MN, Yang WM, Yan H, Zhang C, An Y, Zhang FH (2020) Experimental investigation of flame retardancy and mechanical properties of APP/EG/TPU multilayer composites prepared by microlayer coextrusion technology. *J Appl Polym Sci* 138(5):50219
 17. Tang G, Jiang HH, Yang YD, Chen DP, Liu CL, Zhang P, Zhou L, Huang XJ, Zhang H, Liu XY (2020) Preparation of melamine-formaldehyde resin-microencapsulated ammonium polyphosphate and its application in flame retardant rigid polyurethane foam composites. *J Polym Res* 27(12):375
 18. Chen LY, Wu WH, Meng WH, Xu S, Han HD, Yu YF, Qu HQ, Xu JZ (2018) Application of metallic phytates to poly(vinyl chloride) as efficient biobased phosphorous flame retardants. *J Appl Polym Sci* 135(33):46601
 19. Mu XW, Pan Y, Ma C, Zhan J, Song L (2018) Novel Co₃O₄/covalent organic frameworks nanohybrids for conferring enhanced flame retardancy, smoke and CO suppression and thermal stability to polypropylene. *Mater Chem Phys* 215:20–30
 20. Yuan Y, Ma C, Shi YQ, Song L, Hu Y, Hu WZ (2018) Highly-efficient reinforcement and flame retardancy of rigid polyurethane foam with phosphorus-containing additive and nitrogen-containing compound. *Mater Chem Phys* 211:42–53
 21. Modesti M, Lorenzetti A, Besco S, Hrelja D, Semenzato S, Bertani R, Michelin RA (2008) Synergism between flame retardant and modified layered silicate on thermal stability and fire behaviour of polyurethane nanocomposite foams. *Polym Degrad Stabil* 93(12):2166–2171
 22. Wu K, Zhang YK, Hu WG, Lian JT, Hu Y (2013) Influence of ammonium polyphosphate microencapsulation on flame retardancy, thermal degradation and crystal structure of polypropylene composite. *Compos Sci Technol* 81:17–23
 23. Guo WW, Wang X, Zhang P, Liu JJ, Song L, Hu Y (2018) Nanofibrillated cellulose-hydroxyapatite based composite foams with excellent fire resistance. *Carbohydr Polym* 195:71–78
 24. Huang YB, Jiang SH, Liang RC, Sun P, Hai Y, Zhang L (2020) Thermal-triggered insulating fireproof layers: A novel fire-extinguishing MXene composites coating. *Chem Eng J* 391:123621
 25. Shi YQ, Liu C, Duan ZP, Yu B, Liu MH, Song PG (2020) Interface engineering of MXene towards super-tough and strong polymer nanocomposites with high ductility and excellent fire safety. *Chem Eng J* 339:125829
 26. Sun LS, Qu YT, Li SX (2013) Co-microencapsulate of ammonium polyphosphate and pentaerythritol in intumescent flame-retardant coatings. *J Therm Anal Calorim* 11(2):1099–1106
 27. Prabhakar MN, Raghavendra GM, Vijaykumar BVD, Patil K, Seo J, Jung-il S (2019) Synthesis of a novel compound based on chitosan and ammonium polyphosphate for flame retardancy applications. *Cellulose* 26(12):1–12
 28. Jiang ZL, Wang CS, Fang SY, Ji P, Wang HP, Ji CC (2018) Durable flame-retardant and antidroplet finishing of polyester fabrics with flexible polysiloxane and phytic acid through layer-by-layer assembly and sol-gel process. *J Appl Polym Sci* 135(27):46414
 29. Jin SL, Qian LJ, Qiu Y, Chen YJ, Xin F (2019) High-efficiency flame retardant behavior of bi-DOPO compound with hydroxyl group on epoxy resin. *Polym Degrad Stabil* 166:344–352
 30. Wang X, Zhang P, Huang ZC, Xing WY, Song L, Hu Y (2019) Effect of aluminum diethylphosphinate on the thermal stability and flame retardancy of flexible polyurethane foams. *Fire Saf J* 106:72–79
 31. Ma D, Zhao PH, Li J (2017) Effects of zinc phytate on flame retardancy and thermal degradation behaviors of intumescent flame-retardant polypropylene. *Polym Plast Technol Eng* 56(11):1167–1176
 32. Wu ZH, Wang Q, Fan QX, Cai YJ, Zhao YQ (2018) Synergistic effect of Nano-ZnO and intumescent flame retardant on flame retardancy of polypropylene/ethylene-propylene-diene monomer composites using elongational flow field. *Polym Compos* 40(7):2819–2833
 33. Chen HB, Shen P, Chen MJ, Zhao HB, Schiraldi DA (2016) Highly efficient flame retardant polyurethane foam with alginate/clay aerogel coating. *ACS Appl Mater Interfaces* 8(47):32557–32564
 34. Liu C, Wu W, Shi YQ, Yang FQ, Liu MH, Chen ZX, Yu B, Feng YZ (2020) Creating MXene/reduced graphene oxide hybrid towards highly fire safe thermoplastic polyurethane nanocomposites. *Compos Part B Eng* 203:108486
 35. Wang D, Zhang QJ, Zhou KQ, Yang W, Hu Y, Gao XL (2014) The influence of manganese-cobalt oxide/graphene on reducing fire hazards of poly(butylene terephthalate). *J Hazard Mater* 278:391–400
 36. Cai W, Wang BB, Liu LX, Zhou X, Chu FK, Zhan J, Hu Y, Kan YC, Wang X (2019) An operable platform towards functionalization of chemically inert boron nitride nanosheets for flame retardancy and toxic gas suppression of thermoplastic polyurethane. *Compos Part B Eng* 178:107462
 37. Xu XK, Pan RM, Li P, Chen RY (2020) Kinetics, Thermodynamics, and volatile products of camphorwood pyrolysis in inert atmosphere. *Appl Biochem Biotechnol* 191(4):1605–1623
 38. Zhao B, Liu DY, Liang WJ, Li F, Wang JS, Liu YQ (2017) Bi-phase flame-retardant actions of water-blown rigid polyurethane

- foam containing diethyl-N, N-bis(2-hydroxyethyl) phosphoramidate and expandable graphite. *J Anal Appl Pyrolysis* 124:247–255
39. Huang YB, Jiang SH, Liang R C, Liao ZW, You GX (2019) A green highly-effective surface flame-retardant strategy for rigid polyurethane foam: Transforming UV-cured coating into intumescent self-extinguishing layer. *Compos Part A Appl S* 125:105534
 40. Xu ZS, Deng N, Yan L, Chu ZY (2018) Functionalized multi-walled carbon nanotubes with monocomponent intumescent flame retardant for reducing the flammability and smoke emission characteristics of epoxy resins. *Polym Adv Technol* 29(12):3002–3013
 41. Yang HY, Wang X, Song L, Bin Y, Yuan Y, Hu Y, Yuen RKK (2014) Aluminum hypophosphite in combination with expandable graphite as a novel flame retardant system for rigid polyurethane foams. *Polym Adv Technol* 25(9):1034–1043
 42. Wang X, Zhou S, Xing WY, Yu B, Feng XM, Song L, Hu Y (2013) Self-assembly of Ni-Fe layered double hydroxide/graphene hybrids for reducing fire hazard in epoxy composites. *J Mater Chem A* 1(13):4383–4390
 43. Liu C, Zhang P, Shi YQ, Rao XH, Cai SC, Fu LB, Feng YZ, Wang LC, Zheng XQ, Wei Yang (2020) Enhanced fire safety of rigid polyurethane foam via synergistic effect of phosphorus/nitrogen compounds and expandable graphite. *Molecules* 25(20):4741

Publisher's Note Springer Nature remains neutral with regard to jurisdictional claims in published maps and institutional affiliations.